

Formation of large-scale magnetic structures associated with the *Fermi* bubbles

M. V. Barkov^{1,2} and V. Bosch-Ramon³

¹ Max-Planck-Institut für Kernphysik, Saupfercheckweg 1, 69117 Heidelberg, Germany; bmv@mpi-hd.mpg.de

² Space Research Institute RAS, 84/32 Profsoyuznaya Street, Moscow, 117997, Russia

³ Departament d'Astronomia i Meteorologia, Institut de Ciències del Cosmos (ICC), Universitat de Barcelona (IEEC-UB), Martí i Franquès 1, 08028 Barcelona, Spain, e-mail: vbosch@am.ub.es

Received ;date; / Accepted ;date;

ABSTRACT

Context. The *Fermi* bubbles are part of a complex region of the Milky Way. This region presents broadband extended non-thermal radiation, apparently coming from a physical structure rooted in the Galactic Centre and with a partly-ordered magnetic field threading it.

Aims. We explore the possibility of an explosive origin for the *Fermi* bubble region to explain its morphology, in particular that of the large-scale magnetic fields, and provide context for the broadband non-thermal radiation.

Methods. We perform 3D magnetohydrodynamical simulations of an explosion from a few million years ago that pushed and sheared a surrounding magnetic loop, anchored in the molecular torus around the Galactic Centre.

Results. Our results can explain the formation of the large-scale magnetic structure in the *Fermi* bubble region. Consecutive explosive events may match better the morphology of the region. Faster velocities at the top of the shocks than at their sides may explain the hardening with distance from the Galactic Plane found in the GeV emission.

Conclusions. In the framework of our scenario, we estimate the lifetime of the *Fermi* bubbles as $\approx 2 \times 10^6$ yr, with a total energy injected in the explosion(s) $\gtrsim 10^{55}$ ergs. The broadband non-thermal radiation from the region may be explained by leptonic emission, more extended in radio and X-rays, and confined to the *Fermi* bubbles in gamma rays.

Key words. Shock waves, Methods: numerical, Galaxy: center

1. Introduction

Originating in the Galactic Centre and extending up to a distance of ≈ 15 kpc from the Galactic plane, there is a large bipolar structure with counterparts in different wavelengths, from radio to gamma rays. This structure was seen for the first time by *ROSAT* in X-rays (Snowden et al., 1997). An overlapping extended source was also detected in radio by WMAP (Finkbeiner, 2004), and a few years later *Fermi* detected a somewhat smaller structure in the GeV range, the *Fermi* bubbles, with a height of ≈ 8 kpc (Su et al., 2010a). A hint of an extension of the GeV emission beyond the *Fermi* bubbles was also been found on scales similar to those of the *ROSAT* emission (Ackermann et al., 2012). S-PASS (Carretti et al., 2013) and WMAP (Jones et al., 2012) detected a large-scale, partly-ordered magnetic-field structure placed at $20^\circ - 50^\circ$ from the galactic plane in the *Fermi* bubble region, but larger than the bubbles themselves.

The origin of the *Fermi* bubbles is still under debate. There are two main hypothesis, which were already raised in Su et al. (2010a): active galactic nucleus (AGN) activity, or a bipolar galactic wind. In fact, a combined origin of central accretion activity and a galactic wind fed by star formation may be possible, as discussed in Carretti et al. (2013). In that work, the authors adopted a leptonic sce-

nario for the *Fermi* bubbles emission, whereas Crocker & Aharonian (2011) considered hadronic radiation.

Numerical simulations of the dynamics of the *Fermi* bubbles can be useful to unveil relevant physical processes underlying the detected radiation. In this regard, numerical hydrodynamical simulations of the *Fermi* bubbles were performed in 2D (Guo & Mathews, 2012; Guo et al., 2012) and 3D (Yang et al., 2012). In the latter paper, the authors took into account anisotropic diffusion of cosmic rays to explain the sharp edges of the *Fermi* bubbles in gamma rays. In Guo & Mathews (2012), the X-rays detected by *ROSAT* were explained as thermal radiation from the surrounding medium heated by a shock, and the gamma rays from the *Fermi* bubbles as coming from relativistic electrons in the ejecta.

Specially motivated by the recent detection of a partly-ordered magnetic-field structure in the *Fermi* bubble region, this work presents the results of 3D magnetohydrodynamical (MHD) simulations of the structures associated with the *Fermi* bubbles in the framework of a mini-AGN event in which material is ejected from the central Galactic black hole (see Bland-Hawthorn et al., 2013, for recent observational support for the AGN scenario). We interpret in this context the recent observational findings in radio, in particular concerning the large-scale magnetic field, and suggest a non-thermal nature of the X-ray radiation detected by *ROSAT* that would be produced by electrons accelerated in the shock driven by the ejecta in the surrounding medium. The GeV emission from the *Fermi* bub-

Send offprint requests to: M. V. Barkov, e-mail: bmv@mpi-hd.mpg.de

arXiv:1311.6722v1 [astro-ph.HE] 26 Nov 2013

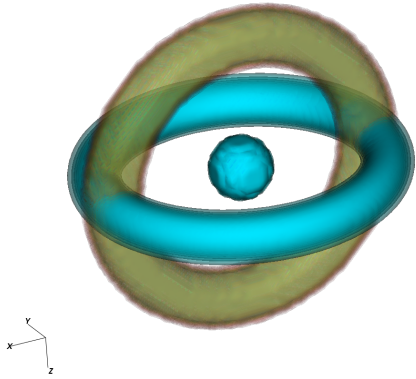


Fig. 1. The sketch of the initial configuration: the opaque horizontal torus is a gaseous disc with total radius $R_D = 1$ kpc and *small* radius $r_D = 0.2$ kpc; the translucent vertical ring is a magnetic loop with the same radius and thickness as those of the gaseous disc. The central sphere of radius $r_s = 0.2$ kpc represents a central region with high pressure and velocity: the ejection region.

bles could result from particle acceleration in the shock wave of a second explosive event in a recurrent-activity scenario, or particle acceleration within the ejecta, in which shocks, turbulence, and suitable conditions for magnetic reconnection are present. All through the paper, the notation $A_b = A/10^b$ has been adopted, where A has cgs units.

2. Physical scenario

We present an MHD model for the formation of the large-scale magnetic-field structure in the *Fermi* bubble region in the context of accretion-driven explosive events. The evolution and observational properties of the *Fermi* bubbles and accompanying structures can be strongly influenced by the presence of this large-scale magnetic field.

We assume that the very central region of the Galaxy is surrounded by a rotating gaseous torus or disc with total radius R_D , effective thickness or *small* radius of the torus r_D , and rotation speed v_D . Loops of magnetic field thread the central region. These magnetic loops, of strength B_1 , are anchored in the disc and surround the central region as shown in Fig. 1.

In the proposed scenario, the formation of the *Fermi* bubble region goes as follows. A molecular disc, with a lifetime $\sim 10^7$ years (Molinari et al., 2011), surrounds the Galactic Centre. A magnetic field loop anchored in the disc also crosses the disc polar regions. At a given time, and possibly episodically, the accretion rate in the central black hole increases dramatically due for instance to the capture of a molecular cloud. Such an accretion event can launch a powerful outflow in the polar direction, as it happens in AGN. The ejecta will stretch the magnetic field loops crossing the polar regions, and push the external medium up- and side-wards, shocking it. Simultaneously, the external layers of the whole structure, where the ejecta and the external medium are in contact, will be twisted by the rotating gaseous disc through the surrounding magnetic field anchored to the disc and sheared as well by differential rotation. As shown below, this scenario can produce the partly-ordered magnetic-field structure similar to that found in S-PASS.

3. Simulations

The simulations presented here were implemented in 3D Cartesian geometry using the *PLUTO* code (Mignone et al., 2007, 2012), the piece-parabolic method (PPM) (Colella & Woodward, 1984; Mignone et al., 2005), an HLLD Riemann Solver (Miyoshi & Kusano, 2008), and applying AMR using the *Chombo* code (Colella et al., 2009). The flow was approximated as an ideal, adiabatic gas with magnetic field, one particle species, and polytropic index of 5/3. The adopted resolution was $48 \times 48 \times 96$ cells and 3 levels of AMR, which gives an effective resolution of $384 \times 384 \times 768$ cells. The size of the domain was $x \in [0, 18 \text{ kpc}]$, $y \in [0, 18 \text{ kpc}]$, and $z \in [0, 36 \text{ kpc}]$. The calculations were carried out in the Moscow State University cluster *Chebyshev*. The visualization of the results were arranged with *VisIt*.

3.1. Initial setup

In the centre of our galaxy there is a massive gaseous disc of $\sim 3 \times 10^7 M_\odot$, a radius of 100 pc, and a rotation speed $\sim 80 \text{ km s}^{-1}$ (see Molinari et al., 2011). The simulation initial configuration sets an horizontal gaseous torus in the plane XY (the disc), and a vertical magnetic field loop in the plane XZ . The torus radius and effective thickness are taken $R_D = 1$ kpc and $r_D = 0.2$ kpc, respectively. We fix the central particle density of the torus to 10^3 cm^{-3} , and assume constant angular momentum and hydrostatic equilibrium to determine the torus pressure and temperature distribution. We use a truncated Keplerian gravitational potential $\phi \propto 1/\max(r, 0.6\text{kpc})$. Such a potential will not significantly influence the calculation results because the speed of the shock wave at all radii is significantly larger than the escape velocity. The magnetic loop radius and thickness are taken equal to those of the torus (see Fig.1). The initial strength of the magnetic field in the loop is $100 \mu\text{G}$, similar to the observed value in the Galactic center (Crocker et al., 2010, 2011). Numerical limitations have led us to adopt a larger size of the disc/torus and the associated magnetic loop. This has also implied that the disc is simulated rotating in the gravitational potential of the central region with a rather high speed, $v_D = 800 \text{ km/s}$, to have a disc angular velocity equal to the actual angular velocity of the molecular disc in the center of the Galaxy. Hence, in practice, the main difference between our simulation and a more realistic setup is the width of the inner ejection region, which is expected to have a minor impact on the long-term evolution of the simulated structures. In addition, the somewhat unrealistic torus properties do not allow a precise, quantitative comparison between the simulated magnetic-field strength and the observed values. However, given that the magnetic field is not dynamically relevant, it is determined by the fluid evolution and the obtained global field geometry should be reliable. The lifetime of the central engine activity is assumed to be much shorter than the disc or the dynamical scale of the simulation.

The explosive activity produces an axial outflow from a central sphere of radius $r_s = 0.2$ kpc. The outflow, initially confined in this sphere, has been set with two different total energies for one simulation with one ejection: $E_{\text{tot}} = 10^{55}$ and 3×10^{55} erg; a particle density of 1 cm^{-3} , and a velocity of $v_e = 3.5 \times 10^9 \text{ sign}(z) E_{56}^{1/2} \text{ cm s}^{-1}$ at ejection, being directed along the Z -axis. The gas density of the surrounding medium is set as in Miller & Bregman (2013):

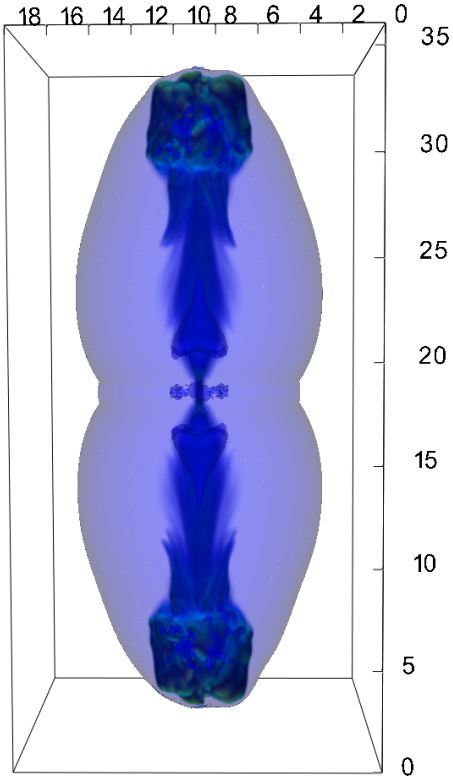


Fig. 3. The distribution of the ejected matter tracer (opaque blue-green) and pressure surface (transparent magenta) indicates the position of the shock wave from the model with $E_{\text{tot}} = 3 \times 10^{55}$ erg at $t = 2.3$ Myr.

$n_{\text{bg}} = \frac{n_0}{[1+(R/R_C)^2+(z/z_C)^2]^{3\beta/2}}$, where $n_0 = 0.46 \text{ cm}^{-3}$, R is the cylindrical radius, z the distance from the Galactic plane, and $\beta = 0.71$, $R_C = 0.42 \text{ kpc}$ and $z_C = 0.26 \text{ pc}$ are normalizing constants. The temperature of this medium is fixed to $1.2 \times 10^6 \text{ K}$. Provided that accretion events may be recurrent, we have performed an additional simulation with two active episodes. An amount of energy $E_{\text{tot}} = 10^{55}$ erg was now twice injected, at $t = 0$ and at $t = 2.5$ Myr. The central engine activity was taken shorter than the flow crossing time, $r_s/v_e \sim 10^4 \text{ yr}$. Being much shorter than any relevant dynamical process in the simulation, the activity periods can indeed be considered as discrete events. Note that the formation timescale of this magnetic field structure is $\sim 100 \text{ pc}/80 \text{ km s}^{-1} \approx 1 \text{ Myr}$, which implies that the magnetic loop can keep being generated between events.

3.2. Results

The distributions of velocity and magnetic-field lines are presented in Fig. 2 for two models, $E_{\text{tot}} = 3 \times 10^{55}$ and $E_{\text{tot}} = 10^{55}$ erg, at the time when the size along the Z -direction of the whole structure reached $\approx 15 \text{ kpc}$. The expansion of the high-pressure region blows up the bubbles and stretches the magnetic-field lines, and meanwhile the rotation of the magnetic-line foot points twist the magnetic field into a spiral structure. This spiral structure is similar to that observed in Carretti et al. (2013).

The ejected matter from the central engine forms a bipolar, elongated and wide structure. The shock wave traveling through the Galactic halo forms an external bubble of shocked external medium almost as wide as long.

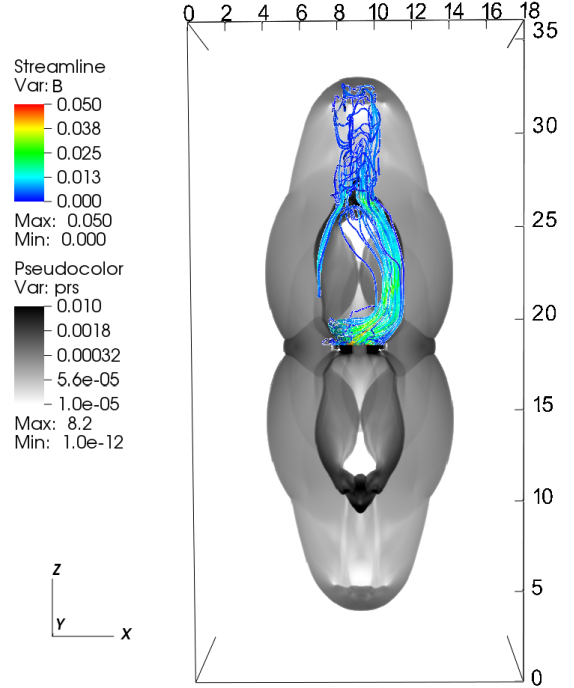


Fig. 4. The distribution of the gas pressure (bottom and top) and magnetic-field lines (top) at $t = 3.4$ Myr for a model with two active episodes, with $E_{\text{tot}} = 10^{55}$ erg each at times $t = 0$ and $t = 2.5$ Myr. The pressure is presented in units of 1.67×10^{-8} pa and the magnetic field (shown by colour) in units of $400 \mu\text{G}$.

Surrounded by this shocked external medium, the ejected matter forms a narrower second bubble with its neck at the Galactic Centre (see Fig. 3). Covering the inner bubble, at the contact layer between the ejecta and the shocked external medium, the pushed magnetic field is threaded, sheared and anchored in the rotating disc. The magnetic structure induces minor perturbations on the contact layer. In the simulation with two active episodes a second bubble forms inside the first one, as shown in Fig. 4. In this case, the sheared magnetic lines anchored in the molecular disc surround the shock wave formed by the second bubble on the earlier one. An interesting property of the computed solution is a higher speed at the top of the bubble shocks than at their sides. This effect is produced by a decreasing background-density profile.

4. Discussion

In this work we propose an accretion-ejection, explosive scenario for the formation of the large-scale magnetic-field structure around the *Fermi* bubbles. As shown in Fig. 3, one explosion produces very extended ejecta, much larger than the *Fermi* bubbles themselves, with the head reaching up to the external boundary of the whole structure. This mismatch in size may be explained by invoking acceleration and confinement of the GeV emitting particles only deep into the ejecta. Another possibility would come from accretion-ejection events recurrent on timescales $\gtrsim 10^6 \text{ Myr}$. Such a timescale, and the energetics derived here, would imply an average injection luminosity of $\sim 10^{41} \text{ erg s}^{-1}$, compatible with cosmic ray injection. As shown in Fig. 4, the two-episodes scenario, with such

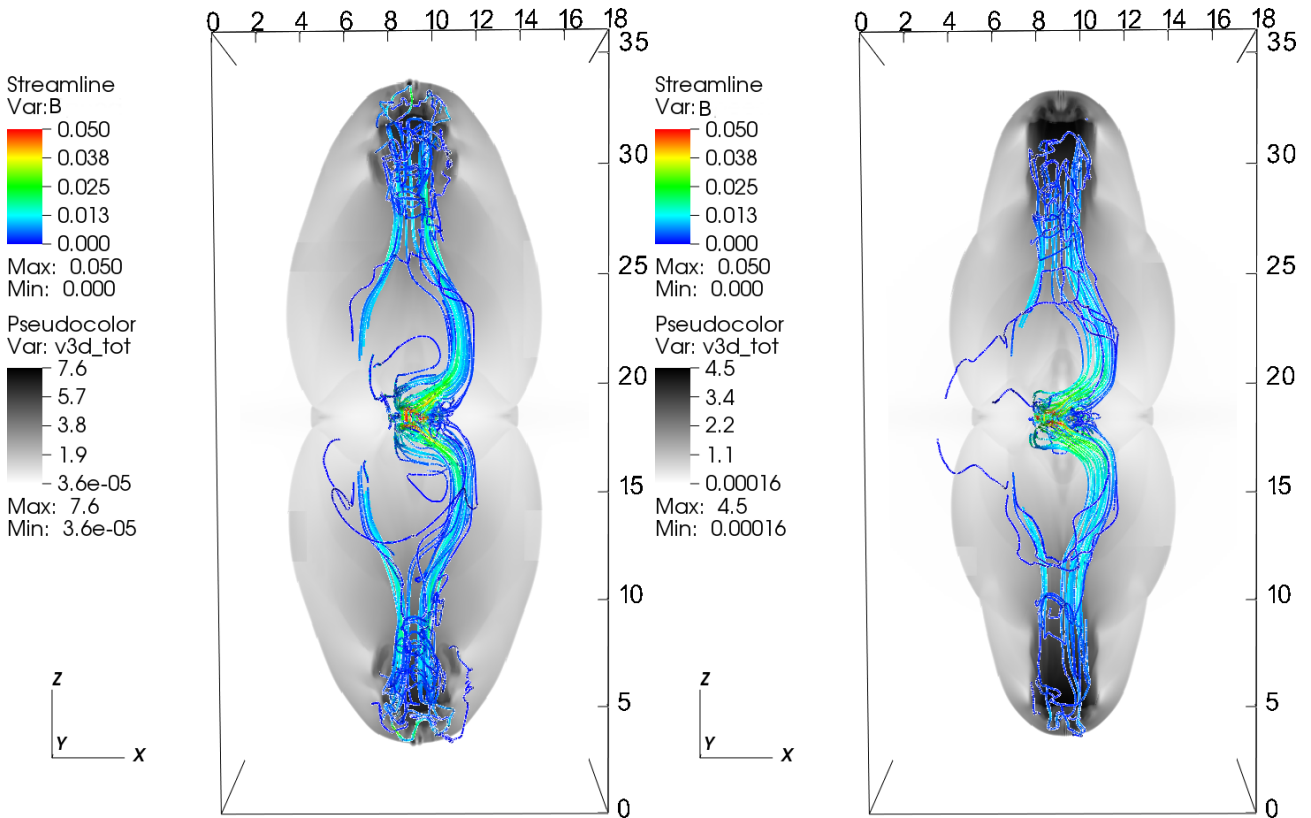


Fig. 2. The distribution of the gas velocity modulus and the magnetic-field lines for two models: on the left panel, $E_{\text{tot}} = 3 \times 10^{55}$ erg at a time $t = 2.3$ Myr; on the right panel, $E_{\text{tot}} = 10^{55}$ erg at $t = 3.4$ Myr. The velocity is presented in units of 10^8 cm/s and the magnetic-field strength (shown by colour) in units of $400 \mu\text{G}$.

a characteristic timescale and energy budget, nicely reproduces the overall morphology of the whole *Fermi* bubble region, in particular the sharp edge of the *Fermi* bubbles themselves¹. It is worth noting that, independently of the simulation, the assumption of a magnetic structure anchored in the central molecular disc already provides a constraint on the age of the *Fermi* bubbles, $\lesssim 10^7$ yr. If it were true, such a short lifetime would disfavor the hadronic scenario. This is so because of the long cooling time of proton-proton collisions (Kelner et al., 2006): $t_{\text{pp}} = 10^{15}/n > 10^{18}n_{-4}^{-1}$ sec = $3 \times 10^{10}n_{-4}^{-1}$ yr, $\sim 10^4$ times longer than the dynamical time of the magnetic field. This low efficiency would require a total energy only in high energy protons $\sim L_{\gamma}t_{\text{pp}}/0.17 = 2 \times 10^{56}$ ergs, 10 times larger than the total energetics of the *Fermi* bubbles if they are related to the large-scale magnetic-field structure, as assumed here. Accounting for dynamical constraints, i.e. to explain the growth of the structure in the surrounding medium on the timescales considered here, one gets an estimate on the luminosity injected into the *Fermi* bubbles of $\sim 10^{41}$ ergs. This is $\sim 10^3$ times larger than the energy required to explain the gamma-ray luminosity, so the energy budget is not tight when considering a leptonic origin of the gamma-ray emission.

Let us now briefly consider a framework for the broadband detected radiation. Electrons and protons can be accelerated at the shock produced by the ejected matter in

the surrounding medium. As just argued, protons are disfavored by the relatively short timescales involved in the adopted scenario. For electrons, on the other hand, this is not a problem, with the most efficient radiation process at low energies being synchrotron, and at high energies, inverse Compton (IC) with soft Galactic photons of ~ 1 eV. The maximum energy of the photons produced via synchrotron from shock accelerated electrons can be estimated as $\epsilon_s \approx 0.12(v_{s,8})^2 \eta^{-1}$ keV (Aharonian & Atoyan, 1999), where v_s is the forward-shock speed. However, given the slow steepening with energy above ϵ_s of the synchrotron spectrum of shock accelerated electrons (Zirakashvili & Aharonian, 2007), the effective maximum energy of the synchrotron photons may be estimated about $10 \times \epsilon_s$. With a speed of the shock wave of $\sim 2 \times 10^8$ cm s⁻¹, synchrotron X-rays can reach up to few keV. This synchrotron radiation could explain the X-ray shell or arch found by ROSAT (Snowden et al., 1997), which would have then a non-thermal origin instead of a thermal one (both possibilities were discussed for instance in Su et al., 2010b); IC emission from the same electrons could explain the hint of GeV radiation found on similar scales (see fig. 6 in Ackermann et al. 2012). A diffuse lower-energy electron population, extended also beyond the *Fermi* bubbles but partially embedded in the spiral-like magnetic lines, could explain the WMAP extended source. The *Fermi* bubbles themselves would have an IC origin. They would remain confined to the fresher material of the most recent episode, or alternatively, to deeper regions of the whole region if only one explosion took place as it was discussed by Guo & Mathews (2012). A hardening of the GeV radiation along the Z -direction has been

¹ Such an explanation for the sharp edge of the *Fermi* bubbles is only valid as long as the bubbles and the structures at larger scales have a common origin.

observed for the *Fermi* bubbles (Hooper & Slatyer, 2013). This hardening could be explained by the varying speed of the bubble shocks mentioned in Sect. 3.2, affecting (at least slightly) the slope of the distribution of the GeV emitting particles. This hardening may also be consistent with a stronger shock at the top of the bubbles than at their sides.

Acknowledgements. We want to thank the anonymous referee for useful and constructive comments. The calculations were carried out in the cluster of Moscow State University *Chebyshev*. We thank Andrea Mignone and the *PLUTO* team for the possibility to use the *PLUTO* code. We also thank the *Chombo* team for the possibility to use the *Chombo* code. We would like to thanks to *VisIt* visualization packet team. BMV acknowledges partial support by RFBR grant 12-02-01336-a. V.B.R. acknowledges support by DGI of the Spanish Ministerio de Economía y Competitividad (MINECO) under grants AYA2010-21782-C03-01 and FPA2010-22056-C06-02. V.B.R. acknowledges financial support from MINECO through a Ramón y Cajal fellowship. This research has been supported by the Marie Curie Career Integration Grant 321520.

References

- Ackermann, M., Ajello, M., Atwood, W. B., et al. 2012, ApJ, 750, 3
 Aharonian, F. A. & Atoyan, A. M. 1999, A&A, 351, 330
 Bland-Hawthorn, J., Maloney, P., Sutherland, R., & Madsen, G. 2013, ArXiv:1309.5455
 Carretti, E., Crocker, R. M., Staveley-Smith, L., et al. 2013, Nature, 493, 66
 Colella, P., Graves, D. T., Keen, N. D., et al. 2009, Library, 42
 Colella, P. & Woodward, P. R. 1984, Journal of Computational Physics, 54, 174
 Crocker, R. M. & Aharonian, F. 2011, Physical Review Letters, 106, 101102
 Crocker, R. M., Jones, D. I., Aharonian, F., et al. 2011, MNRAS, 413, 763
 Crocker, R. M., Jones, D. I., Melia, F., Ott, J., & Protheroe, R. J. 2010, Nature, 463, 65
 Finkbeiner, D. P. 2004, ApJ, 614, 186
 Guo, F. & Mathews, W. G. 2012, ApJ, 756, 181
 Guo, F., Mathews, W. G., Dobler, G., & Oh, S. P. 2012, ApJ, 756, 182
 Hooper, D. & Slatyer, T. R. 2013, ArXiv:1302.6589
 Jones, D. I., Crocker, R. M., Reich, W., Ott, J., & Aharonian, F. A. 2012, ApJ, 747, L12
 Kelner, S. R., Aharonian, F. A., & Bugayov, V. V. 2006, Phys. Rev. D, 74, 034018
 Mignone, A., Bodo, G., Massaglia, S., et al. 2007, ApJS, 170, 228
 Mignone, A., Plewa, T., & Bodo, G. 2005, ApJS, 160, 199
 Mignone, A., Zanni, C., Tzeferacos, P., et al. 2012, ApJS, 198, 7
 Miller, M. J. & Bregman, J. N. 2013, ApJ, 770, 118
 Miyoshi, T. & Kusano, K. 2008, in Astronomical Society of the Pacific Conference Series, Vol. 385, Numerical Modeling of Space Plasma Flows, ed. N. V. Pogorelov, E. Audit, & G. P. Zank, 279
 Molinari, S., Bally, J., Noriega-Crespo, A., et al. 2011, ApJ, 735, L33
 Snowden, S. L., Egger, R., Freyberg, M. J., et al. 1997, ApJ, 485, 125
 Su, M., Slatyer, T. R., & Finkbeiner, D. P. 2010a, ApJ, 724, 1044
 Su, M., Slatyer, T. R., & Finkbeiner, D. P. 2010b, ApJ, 724, 1044
 Yang, H.-Y. K., Ruszkowski, M., Ricker, P. M., Zweibel, E., & Lee, D. 2012, ApJ, 761, 185
 Zirakashvili, V. N. & Aharonian, F. 2007, A&A, 465, 695